Retrieving Angular Distributions of High-Order Harmonic Generation from a Single Molecule

Kazumichi Yoshii, Godai Miyaji, and Kenzo Miyazaki*

Advanced Laser Science Research Section, IAE, Kyoto University Uji, Kyoto 611-0011, Japan

(Received 6 August 2010; published 7 January 2011)

We present a novel method to retrieve angular distributions of high-order harmonic generation from a single molecule. This technique uses an iterative procedure based only on experimental results of time and angle-dependent harmonic signals, and no actual shape of molecular orbital is assumed. The molecular axis distribution in a target gas can simultaneously be deduced in this procedure. The angle-dependent signal retrieved for a single N_2 and O_2 molecule is demonstrated to reflect the highest occupied molecular orbital, excluding the ambiguity due to the imperfect alignment.

DOI: 10.1103/PhysRevLett.106.013904 PACS numbers: 42.65.Ky, 33.80.Rv, 33.90.+h

High-order harmonic generation (HHG) from nonadiabatically aligned molecules [1,2] provides an effective tool for measuring structures and dynamics of gas phase molecules [3–10]. In aligned molecules, the HHG is very sensitive to the molecular orbital and its spatial orientation with respect to the incident field polarization. Owing to the sensitivity, this technique has represented rich advantages in the study of strong-field interactions with molecules, such as molecular wave packet dynamics [3,4], imaging molecular orbital structures [5,6], and manipulating harmonic phase and polarization [7–9]. Furthermore, the HHG in aligned molecules has recently attracted increasing attention to understand ultrafast electron dynamics in multiple orbitals on attosecond and angstrom scales [10–12].

The unique functions of HHG in molecules certainly rely on the spatial nonuniformity created by the molecular alignment [13,14] in a pump-probe experiment, where the pump pulse aligns molecules while the probe generates the harmonic emission from molecules. Then, the angle-dependent harmonic yield around the molecular axis is the key to deduce structural and dynamic effects of a single molecule [15,16]. Several experiments have been carried out with considerable attention to the angle-dependent harmonic yield [5–9,11,12]. The harmonic distribution observed, however, always includes some broadening of the molecular axis distribution that blurs the structural or orbital shape of a single molecule. This is due to the fact that the HHG is possible only in an ensemble of molecules that can never be perfectly aligned. Thus, a deconvolution procedure concerning the observed harmonic signal is crucial to obtain an angle-dependent harmonic yield for a single molecule [17]. A similar situation is found in the experiment for strong-field ionization of aligned molecules [18].

When an ultrashort laser pulse is used for the nonadiabatic alignment, the spatial distribution of aligned molecules is dominated with the initial rotational temperature T_{rot} [13,14]. For producing low-temperature molecules and a resulting high degree of alignment, a supersonic gas jet has been employed extensively. Then the accurate value of T_{rot} in the interaction region can hardly be predicted mainly due to a rapid spatial gradient of T_{rot} along the beam flow [19], whereas T_{rot} is so important as to characterize HHG from a single molecule [3–12].

In this Letter we report a new method to obtain the angular distribution of harmonic emission produced from *a single molecule*, together with the accurate value of T_{rot} and resulting definite distribution of molecular axes. In this method, where no theoretical assumption is necessary, we use two kinds of harmonic signals observed for an identical harmonic order: one of them is the time-dependent signal produced from coherently rotating molecules under field-free conditions, and the other is the signal measured as a function of the relative angle between pump and probe polarizations at a fixed time delay.

The experimental setup used was the same as in our previous studies [17,19]. Briefly, the linearly polarized, 40 fs, 800 nm pump and probe pulses were produced at a repetition rate of 10 Hz. These pulses were collinearly focused with a 500-mm focal-length lens into a pulsed supersonic molecular beam. The laser intensity in the interaction region was carefully evaluated, since T_{rot} is sensitive to the pump intensity as well as the pulse width. The pulsed molecular beam was jetted into vacuum from a 1-mm diameter nozzle backed with the source gas pressure $P_0 = 1$–6 atm. The distance z_0 between the nozzle exit and the optic axis was varied to change T_{rot} [19]. The harmonic radiation produced was detected by an electron multiplier mounted on a vacuum ultraviolet monochromator.

The time-dependent harmonic signal was measured as a function of the time delay Δt between the pump and probe pulses. The angle-dependent harmonic signal was observed at a fixed time delay Δt by changing the angle α between the polarization directions of the pump and probe pulses, where the pump polarization was rotated while the probe polarization was fixed to the direction along the slit of the monochromator. When the degree of alignment is large, or molecules are highly aligned, the α-dependent harmonic signal at the time delay Δt_{top} for the peak or top alignment should be close to the actual distribution of HHG from a single molecule.

In the present method, we define the time-dependent nth harmonic signal $M^{(n)}_{\mathrm{expt}}(0, \Delta t)$ observed for $\alpha = 0°$ and the α-dependent signal $M^{(n)}_{\mathrm{expt}}(\alpha, \Delta t_{\mathrm{top}})$ observed at Δt_{top}, where the subscript "expt" indicates the experimental value. We use the laboratory coordinates shown in Fig. 1(a) for the polarization directions of pump and probe pulses, the orientation of molecular axis with the polar angle θ, the azimuth angle ϕ, and the relative angle θ' between the molecular axis and the probe polarization. The time-dependent nth harmonic signal $M^{(n)}_{\mathrm{calc}}(\alpha, \Delta t)$ to be calculated for the angle α may be approximated by the relation [20–22]

$$M^{(n)}_{\mathrm{calc}}(\alpha, \Delta t) = \int_{\phi=0}^{2\pi} \int_{\theta=0}^{\pi} \rho(\theta, \phi, \Delta t) S^{(n)}(\theta'(\theta, \phi, \alpha)) \times \sin\theta d\theta d\phi, \tag{1}$$

where the subscript "calc" indicates the calculated value, $\rho(\theta, \phi, \Delta t)$ is the time-dependent distribution of molecular axis, and $S^{(n)}(\theta')$ is the normalized angular distribution of the nth harmonic intensity produced from a single molecule, which we intend to finally deduce from the measurement. Quantum mechanically, $S^{(n)}(\theta')$ is the nth harmonic component in the norm square of the Fourier transform of the induced electronic dipole and should be expressed by a function of α, θ, and ϕ, using the relation $\cos\theta' = \cos\alpha \cos\theta + \sin\alpha \sin\theta \sin\phi$ between θ and θ'. For a value of $\rho(\theta, \phi, \Delta t)$, $S^{(n)}(\theta')$ can be derived with the deconvolution of $M^{(n)}_{\mathrm{calc}}(\alpha, \Delta t_{\mathrm{top}})$ or $M^{(n)}_{\mathrm{calc}}(0, \Delta t)$ that are fitted to the observed signal [18]. The iterative procedure to obtain a self-consistent pair of $\rho(\theta, \phi, \Delta t)$ and $S^{(n)}(\theta')$ may be exemplified as follows for N_2 molecules, where the experiment was carried out at $z_0 = 0.7$ mm with $P_0 = 6$ atm for a low value of T_{rot} [19].

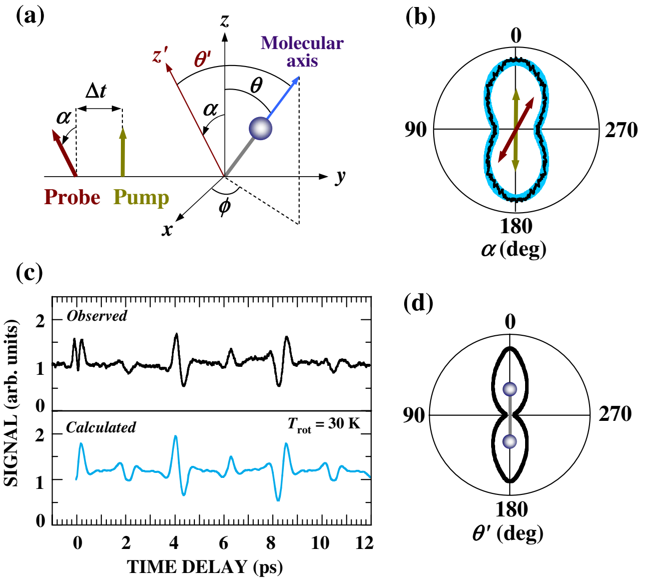

FIG. 1 (color online). Example of high-order harmonic signals retrieved for N_2. (a) Schematic diagram of the laboratory coordinates used in the calculation. (b) The α-dependent 19th harmonic signals observed (narrow black line) and calculated (bold gray line) at Δt_{top}. (c) The time-dependent 19th signals observed (upper trace) and calculated (lower trace) for $\alpha = 0°$. (d) $S^{(19)}(\theta')$ retrieved for a single molecule. The pump and probe intensities used in the experiment are 0.7 and 1.7×10^{14} W/cm^2, respectively. The calculation uses $T_{\mathrm{rot}} = 30$ K for fitting.

We first calculate $\rho(\theta, \phi, \Delta t)$ for a test value of T_{rot} with the time-dependent Schrödinger equation [14] under the same conditions of the pump pulse duration and intensity as in the experiment. Using Eq. (1) with the distribution $\rho(\theta, \phi, \Delta t_{\mathrm{top}})$ obtained, we calculate $S^{(n)}(\theta')$ in the form $S^{(n)}(\theta') = \sum a_m \cos m\theta'$, where the coefficient a_m is determined by fitting $M^{(n)}_{\mathrm{calc}}(\alpha, \Delta t_{\mathrm{top}})$ to the measured signal $M^{(n)}_{\mathrm{expt}}(\alpha, \Delta t_{\mathrm{top}})$. Figure 1(b) shows an example of the calculated 19th harmonic signal $M^{(19)}_{\mathrm{calc}}(\alpha, \Delta t_{\mathrm{top}})$ and compares it with $M^{(19)}_{\mathrm{expt}}(\alpha, \Delta t_{\mathrm{top}})$ observed at $\Delta t_{\mathrm{top}} = 4.00$ ps. The calculated result is in excellent agreement with the experimental.

In this calculation for N_2, we impose two proper restrictions on $S^{(n)}(\theta')$, i.e., $S^{(n)}(\theta') \geq 0$ for the harmonic signal and $dS^{(n)}(\theta')/d\theta' < 0$ $[0 \leq \theta' \leq \pi/2]$. The latter is due to the fact that the observed signal $M^{(n)}_{\mathrm{expt}}(\alpha, \Delta t_{\mathrm{top}})$ would qualitatively be subject to the shape of $S^{(n)}(\theta')$. To confirm the accuracy of $S^{(n)}(\theta')$, we calculate the time-dependent signal $M^{(n)}_{\mathrm{calc}}(0, \Delta t)$ and compare its frequency spectrum with the experimental result, since the spectrum is very sensitive to the rotational distribution in a wave packet [4,15,17]. Figure 1(c) shows an example of $M^{(19)}_{\mathrm{calc}}(0, \Delta t)$ (lower trace) calculated for the 19th harmonic, which is in good agreement with the observed one $M^{(19)}_{\mathrm{expt}}(0, \Delta t)$ (upper trace). When the calculated result is not consistent with the observed result, the calculation is repeated by changing the value of T_{rot}. This iterative procedure can finally produce the harmonic distribution $S^{(n)}(\theta')$ for a single molecule, as presented in Fig. 1(d) for the 19th order.

It is noted that a pair of self-consistent values of $S^{(n)}(\theta')$ and T_{rot} can uniquely be derived from only the measured harmonic signals. The calculation is made with $T_{\mathrm{rot}} = 30$ K, and then the degree of alignment at Δt_{top} is obtained as $\eta_{\mathrm{top}} \equiv \langle\langle\cos^2\theta\rangle\rangle = 0.653$. This value of T_{rot} is consistent with those reported in our previous experiment [19].

The harmonic intensity distribution $S^{(19)}(\theta')$ shown in Fig. 1(d) is certainly subject to the σ_g symmetry of the highest occupied molecular orbital (HOMO) of N_2, which is consistent with those obtained with detailed quantum mechanical calculations [15,16]. Comparing the results of Figs. 1(b) and 1(d), we see that $S^{(19)}(\theta')$ represents a shape sharper than $M^{(19)}_{\mathrm{expt}}(\alpha, \Delta t_{\mathrm{top}})$ along the molecular axis. This is certainly due to the fact that the measurement always includes a blurred angular distribution arising from the imperfect alignment of molecules. This blur is successfully removed for a single molecule, as seen in Fig. 1(d).

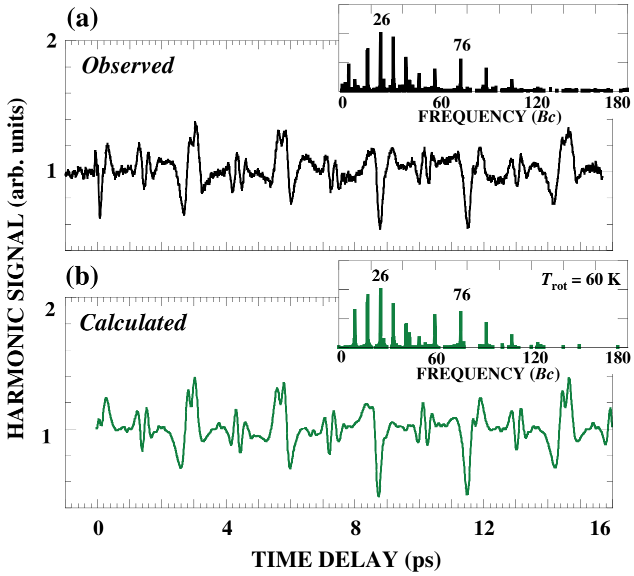

FIG. 2 (color online). Time-dependent 19th harmonic signals (a) observed and (b) retrieved for O_2 as a function of Δt for $\alpha = 0°$, where the insets represent their frequency spectra. The pump and probe intensities used in the experiment are 0.7 and 1.6×10^{14} W/cm^2, respectively. The calculation uses $T_{\mathrm{rot}} = 60$ K for fitting.

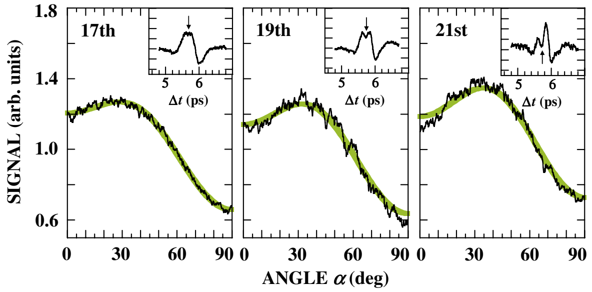

FIG. 3 (color online). Angle-dependent harmonic signals observed (narrow black line) and calculated (bold gray line) for different orders in O_2 at $\Delta t_{\mathrm{top}} = 5.68$ ps. In the insets, the position of Δt_{top} is denoted with an arrow on the time-dependent signal. The conditions for the experiment and calculation are the same in Fig. 2.

To demonstrate the flexibility of the present method, we tried to retrieve the angular distribution of HHG from a single O_2 molecule having a different orbital symmetry. The harmonic generation was made at the position of $z_0 = 1$ mm with $P_0 = 6$ atm, where the lowest value of T_{rot} was observed in our experiment [19]. An example of the measured time-dependent harmonic signals, $M^{(19)}_{\mathrm{expt}}(0, \Delta t)$, is shown in Fig. 2(a), where the inset represents its frequency spectrum. Compared with the upper trace in Fig. 1(c), the signal for O_2 has a double peak structure around Δt_{top}. This characteristic signal arises from the π_g symmetry of HOMO of O_2. The effect of this orbital symmetry on HHG is more clearly seen with the α-dependent harmonic signal $M^{(n)}_{\mathrm{expt}}(\alpha, \Delta t_{\mathrm{top}})$ observed at Δt_{top}, as shown in Fig. 3. The angle-dependent signal for the 17th, 19th, and 21st orders represents a peak around $\alpha = 30°$–$40°$, in contrast with those for N_2. The peak at $0° < \alpha < 90°$ certainly results from the π_g symmetry of O_2.

Based on the observed harmonic signals shown in Figs. 2(a) and 3, we retrieved $S^{(n)}(\theta')$ with the iterative procedure described above. In this calculation, we start with a butterfly-shaped distribution including a peak at $0° < \theta' < 90°$, since the observed α dependence $M^{(n)}_{\mathrm{expt}}(\alpha, \Delta t_{\mathrm{top}})$ would reflect the shape of $S^{(n)}(\theta')$. The calculated result of $M^{(19)}_{\mathrm{calc}}(0, \Delta t)$ is shown in Fig. 2(b), together with the frequency spectrum in the inset. The result reproduces well the observed one including the double peak structure at Δt_{top}, and the frequency spectrum strongly supports the validity of the calculation. In Fig. 3, the calculated α-dependent harmonic signals $M^{(n)}_{\mathrm{calc}}(\alpha, \Delta t_{\mathrm{top}})$ also agree well with the experimental results. The best result is obtained with $T_{\mathrm{rot}} = 60$ K, leading to $\eta_{\mathrm{top}} = 0.574$. This value of T_{rot} higher than that of N_2 is most likely due to the higher cluster population in the gas jet [23].

Figure 4 summarizes the results of $S^{(n)}(\theta')$ obtained for a single O_2 molecule. The angular distributions have a peak around $\theta' = 40°$–$45°$ and nodes at $\theta' = 0°$ and $90°$, which are subject to the π_g symmetry, and the angle for the peak harmonic yield tends to increase with an increase in the harmonic order. These are consistent with the recent theoretical results [15,16]. The sharp angular distribution of HHG from a single O_2 molecule has never been observed in the experiment, as seen in Fig. 3. This is certainly due to the blurred distribution of molecular axes that arises from the partial alignment of molecules. This indicates that the deconvolution of the observed molecular axis distributions is essential to characterize HHG from a single molecule with the π_g symmetry.

The validity of this method was further confirmed by applying $S^{(n)}(\theta')$ obtained for O_2 to the reconstruction of

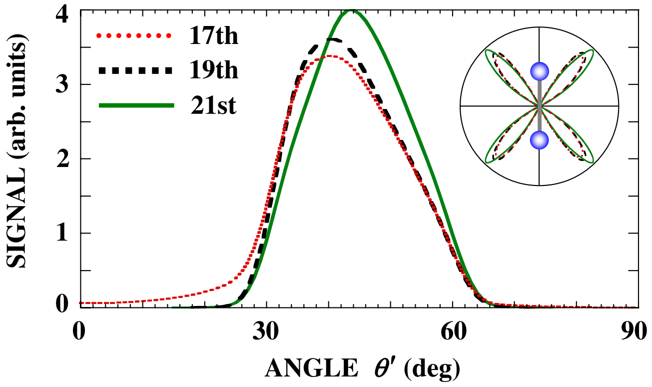

FIG. 4 (color online). Angular distributions of harmonic intensity $S^{(n)}(\theta')$ of different orders retrieved for a single O_2 molecule. The inset represents the polar plots of $S^{(n)}(\theta')$. The conditions for calculation are the same in Fig. 2.

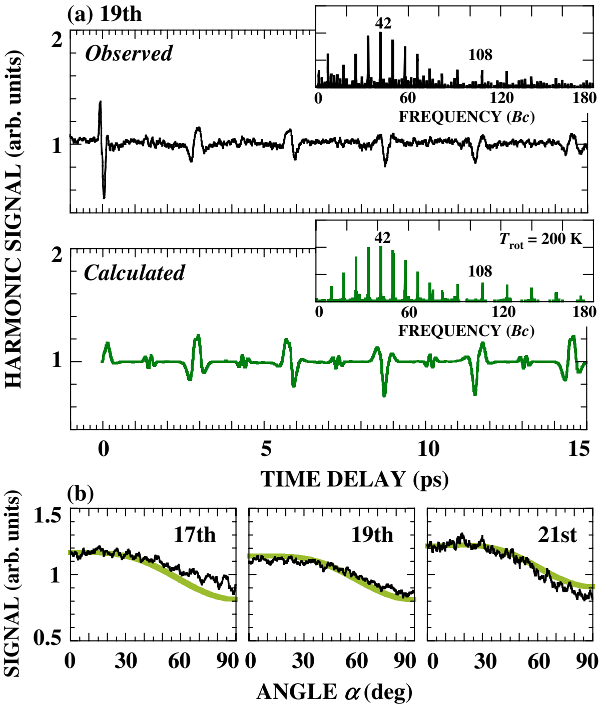

FIG. 5 (color online). Harmonic signals for O_2 at a higher rotational temperature. (a) The time-dependent 19th harmonic signals observed (upper trace) and calculated (lower) for $\alpha = 0°$, where the insets represent their frequency spectra, and (b) the α-dependent signals observed (narrow black line) and calculated (bold gray line) for the 17th, 19th, and 21st orders at $\Delta t_{top} = 5.69$ ps. The pump and probe intensities are the same as in Fig. 2. The calculation uses $T_{rot} = 200$ K for fitting.

the harmonic signal for a different condition of T_{rot}. For this, the HHG was made at $z_0 = 0.1$ mm with $P_0 = 1$ atm, where T_{rot} was expected to be much higher than 60 K [19]. Figure 5 compares the experimental and calculated results, where $T_{rot} = 200$ K is used in the calculation. The calculated results agree well with those observed, and then $\rho(\theta, \phi, \Delta t_{top})$ provides $\eta_{top} = 0.470$ at $\Delta t_{top} = 5.69$ ps. This indicates that one is able to not only retrieve the harmonic distribution for a single molecule but also decode the rotational coherence at an arbitrary value of T_{rot}, once the self-consistent value of $S^{(n)}(\theta')$ is obtained.

In the present method, the accuracy of $S^{(n)}(\theta')$ is mainly dominated with the uncertainty in the pump intensity. For O_2, a 10% change in the intensity was found to produce a shift of 10–15 K in T_{rot}, leading to a change of a few degrees in the peak position of $S^{(n)}(\theta')$. On the other hand, use of Eq. (1) may produce some error owing to the incoherent sum included in $\rho(\theta, \phi, \Delta t)$ [20–22]. We estimated the error and found it small for the harmonic orders concerned [24]. Thus we conclude that the present approach should be useful for the different harmonic orders and molecules, when Eq. (1) approximates well the observed harmonic signal.

In summary, we have shown that the high-order harmonic distribution for a single molecule can be deduced through the iterative procedure, based on only the observed harmonic signals that include the effect of the imperfect alignment. The angular distribution dominated by the HOMO is successfully retrieved for a single N_2 and O_2 molecule, while no actual shape of molecular orbitals is used in the calculation.

---

*miyazaki@iae.kyoto-u.ac.jp

[1] D. Zeidler *et al.*, in *Ultrafast Optics IV*, edited by F. Krausz *et al.* (Springer, New York, 2004), p. 247.
[2] M. Kaku, K. Masuda, and K. Miyazaki, Jpn. J. Appl. Phys. **43**, L591 (2004).
[3] J. Itatani *et al.*, Phys. Rev. Lett. **94**, 123902 (2005).
[4] K. Miyazaki *et al.*, Phys. Rev. Lett. **95**, 243903 (2005).
[5] J. Itatani *et al.*, Nature (London) **432**, 867 (2004).
[6] R. Torres *et al.*, Phys. Rev. Lett. **98**, 203007 (2007).
[7] J. Levesque *et al.*, Phys. Rev. Lett. **99**, 243001 (2007).
[8] X. Zhou *et al.*, Phys. Rev. Lett. **100**, 073902 (2008); **102**, 073902 (2009).
[9] W. Boutu *et al.*, Nature Phys. **4**, 545 (2008).
[10] B. K. McFarland *et al.*, Science **322**, 1232 (2008).
[11] O. Smirnova *et al.*, Nature (London) **460**, 972 (2009).
[12] S. Haessler *et al.*, Nature Phys. **6**, 200 (2010).
[13] F. Rosca-Pruna and M. J. J. Vrakking, Phys. Rev. Lett. **87**, 153902 (2001).
[14] T. Seideman and E. Hamilton, Adv. At. Mol. Opt. Phys. **52**, 289 (2005).
[15] A. Abdurrouf and F. H. M. Faisal, Phys. Rev. A **79**, 023405 (2009).
[16] A.-T. Le *et al.*, Phys. Rev. A **80**, 013401 (2009).
[17] K. Yoshii, G. Miyaji, and K. Miyazaki, Phys. Rev. Lett. **101**, 183902 (2008).
[18] D. Pavicic *et al.*, Phys. Rev. Lett. **98**, 243001 (2007).
[19] K. Yoshii, G. Miyaji, and K. Miyazaki, Opt. Lett. **34**, 1651 (2009).
[20] A.-T. Le, X.-M. Tong, and C. D. Lin, Phys. Rev. A **73**, 041402(R) (2006).
[21] J. P. Marangos *et al.*, J. Mod. Opt. **53**, 97 (2006).
[22] X. X. Zhou *et al.*, Phys. Rev. A **72**, 033412 (2005).
[23] See, e.g., *Atomic and Molecular Beam Methods*, edited by G. Scoles (Oxford University, New York, 1988), Vol. I, pp. 38–53.
[24] To estimate the error arising from the incoherent sum, the α-dependent harmonic signal for O_2 was calculated with the theory that properly considers only the coherent sum for the HHG [15]. The results have shown that the decrease in harmonic signal with an increase in α ($> \sim 40°$) is slightly faster than that in those shown in Fig. 3. This suggests that the present method underestimates the increase in destructive interference with increasing α. The error was less than 15% at $\alpha \sim 90°$, which is comparable to the accuracy in the α-dependent signal measurement. This error from Eq. (1) may become larger, e.g., for such specific cases that the harmonic emission undergoes a large change in polarization states [7,8] or a phase jump [9,11,12], and then some improvement of Eq. (1) and resulting revision of the procedure should be necessary to validate this approach.